Magnetic Properties of Isotropic Polymer Bonded Permanent Magnets Made with Crushed Melt Spun Mixed Rare Earth Iron Boron

Nicholas L. Buelow[1], Iver E. Anderson[2], R.W. McCallum[2], Matthew Kramer[2], Wei Tang[2], Kevin Dennis[2], and Steve Constantinides[3]

[1] Iowa State University, Materials Science and Engineering, 221 Metals Development, Ames, IA 50011

[2] US Dept. of Energy Ames Laboratory, Materials and Engineering Physics, Ames, Iowa, 50011

[3]Arnold Engineering, 300 N. West Street, Marengo, IL 60152

ABSTRACT

Usage of neodymium-iron-boron permanent magnets in sintered and bonded form is growing rapidly as the price of raw materials has declined relative to alternatives. While sintered magnets offer the highest energy output, bonded magnets offer complex shape and magnetization patterns. Bonded magnets are also net shape and can often reduce subsequent assembly steps through insert and multi-component molding. With improvements to the constituent magnetic powders of polymer bonded magnets, useful energy products can be obtained. Of particular interest is the novel mixed rare earth iron boron system ($MRE_2Fe_{14}B$). Melt spun $MRE_2Fe_{14}B$ ribbon can be crushed in an inert environment creating a fine powder that is suitable for polymer bonding. Environmental testing will give insight into the robustness of the magnetic properties and the effect of surface coatings during short and long term exposure to elevated temperature.

INTRODUCTION

Size and weight restrictions influence many engineering designs. Recent permanent magnet (PM) alloy designs have excellent magnetic strength in a small volume, giving a small device the same power as a larger device [1]. The size reduction is the result of PMs with enhanced magnetic properties. Maximum energy product is a measure of the work a PM can do outside its volume. PMs with a high BH_{max} value contain a lot of energy per volume [2]. These new PMs have finely tuned alloy designs and microstructures that directly affect the magnetic properties. Microstructure is the factor limiting the intrinsic capabilities of an alloy design. Several processing methods are used to control the microstructure and therefore optimize the magnetic properties of PMs. Strip casting and grinding [3], melt spinning [4], hydrogen-decomposition-desorption-recombination [5], and gas atomization [6] are processes that can exert good control over the microstructure. The final output of these methods is a PM powder that can be shaped into different types of commercially useful PMs.

Advanced PM powders have two final forms, sintered fully dense and polymer bonded. Sintered fully dense PMs have a high BH_{max}, but are difficult to fabricate into useful shapes due to their brittle nature [7] and are readily attacked by the environment in which they operate [8]. Although much is being done, and has been done, to improve the manufacturability and chemical robustness of sintered fully dense PMs, a polymer bonded magnet (PBM) offers a ready solution to the mechanical, corrosion, and manufacturing issues associated with sintered PMs [9]. The PBM binds the brittle PM powders in a polymer matrix improving the mechanical properties, compared to sintered PMs. The polymer matrix also encapsulates the PM powders effectively separating them from the environment. Net shape manufacturing is possible with PBM as the polymer matrix can be fluidized at temperatures lower than those needed to affect change in the PM microstructure, giving way to injection or compression molding.

PBMs are limited in the BH_{max} value they can reach as compared to sintered fully dense PMs. As a comparison between bonded PMs and sintered PMs, the BH_{max} of a PBM is proportional to the square of the fill factor (f), where the fill factor is the volume percent of PM powder in the PBM, see Eq. 1 [10]. This gives the percentage of BH_{max} the PBM will be able reach as compared to an isotropic sintered fully dense PM.

$$(BH_{max})^{bond} = f^2(BH_{max}) \qquad \text{Equation 1}$$

High loading fractions of PM powders are needed to maximize the BH_{max} of a PBM. PBMs will not be able to compete with sintered magnets in terms of BH_{max}. However, they can offer many other advantages sintered magnets do not offer, compensating for the lack of BH_{max} in other areas that measure the worth of engineering materials.

Rare earth iron boron PM powders have high BH_{max} values and are currently used in high performance PBMs [11]. Of particular interest is novel mixed rare earth iron boron ($MRE_2Fe_{14}B$) PM alloy. This alloy has excellent temperature dependent magnetic properties. $MRE_2Fe_{14}B$ was designed to minimize the loss of BH_{max} as the temperature of the system is increased [11]. Like other commercial $RE_2Fe_{14}B$ PM powders, $MRE_2Fe_{14}B$ was produced via melt spinning which has control parameters that can dictate the microstructure [12]. This process yielded $MRE_2Fe_{14}B$ in an overquenched partially amorphous form that can be annealed to the proper microstructure, optimal for magnetic properties [13].

High temperature polymers are also being considered for use with $MRE_2Fe_{14}B$ powders to maximize the temperature range that the PBMs can operate in. Polyphenylene sulfide (PPS) is a high melting temperature polymer that can be blended with $MRE_2Fe_{14}B$ powder to create a PBM. PPS comes in a powdered form which makes it ideal for blending with $MRE_2Fe_{14}B$ powders.

A major concern when working with any of the rare earth PMs is irreversible loss of magnetic properties that occurs as a result of corrosion [8]. The powders in PBMs are encapsulated in the polymer binder as a result of the fabrication process, but exposure to high temperature can promote deleterious powder surface reactions, in spite of the polymer matrix. Fortunately, the PM powders can also be passivated to further increase their resistance to corrosion. The addition of a passivated layer can be accomplished through the use of a modified fluidized bed process [14] and its effect will be reported.

EXPERIMENTAL PROCEDURE

The $MRE_2Fe_{14}B$ powder was produced via melt spinning which yielded an overquenched partially amorphous ribbon. This ribbon was annealed at 700^0C for 15 minutes to optimize the microstructure. During the annealing process the ribbon was wrapped in a tantalum foil packet and sealed in a quartz vessel at 1/3 atm of ultra high purity helium. More than one melt-spinning run had to be done to produce

enough material for the bonding process. A piece of annealed ribbon was tested from each batch to ensure consistent magnetic properties. After testing the consistency of the magnetic properties, across the entire batch, the ribbon was crushed into a flake form. This was accomplished by placing the annealed ribbon on a 425μm ASTM standard sieve along with ceramic grinding media. Vibration was applied to the sieve, in an inert environment, to promote low energy crushing of the $MRE_2Fe_{14}B$ ribbon. The flake was then blended with an epoxy, and another set blended with PPS.

To protect the $MRE_2Fe_{14}B$ powders from irreversible losses due to corrosion a modified gaseous fluorination process was used to passivate the surface of the powders. The fluorination process is a small batch process, ~7g per run. The powder was sealed in a reaction chamber and heated to ~160ºC in an atmosphere of flowing argon, the carrier gas. To ensure that the flakes are coated evenly they were stirred magnetically. Due to the geometry of the flake powder pure gaseous fluidization is extremely difficult, thus the addition of magnetic stirring. When the particles reached the reaction temperature, ~160ºC, the nitrogen trifluoride (NF_3) reaction gas flow was begun. NF_3 represented only 0.5% of the total gas flow through the chamber.

When the sample had completed the fluorination process a small sample was prepared for thermal gravimetric analysis (TGA), auger, and x-ray photoelectron spectroscopy (XPS) to determine if the coating will be effective in preventing corrosion, as well as, determining thickness and chemical composition of the fluoride coating. Finally, all the powders, treated $MRE_2Fe_{14}B$, untreated $MRE_2Fe_{14}B$, and commercial powders (used as a standard) were bonded with epoxy or PPS for environmental testing.

A set of the bonded PMs were then subjected to a short term irreversible loss test (STILT). This involves pulse magnetization of the bonded PMs and measurement of the Helmholtz flux in the as-bonded state giving a baseline flux for the PBMs. The PBMs are then heated for one hour, in air, at a specified temperature. Then the sample is allowed to cool to room temperature for one hour and the Helmholtz flux is measured again. This process is continued, with a temperature increase each time, to the specified maximum temperature. The final step is to re-saturate the tested PBM to determine the actual irreversible loss due to microstructural degradation.

RESULTS

For the PM powders to retain their magnetic properties, protection from the environment in which they operate is needed. Encapsulating the powder in the polymer matrix of the PBM is effective, generally, in limiting environmental access to the PM powders under normal ambient conditions. However, for applications involving elevated temperatures, for example, another form of protection is, needed, consisting of the addition of a passive layer on each surface of the particle. TGA experiments, Figure 1, subjected passivated and unpassivated $MRE_2Fe_{14}B$, along with two commercial PM powders to a 5ºC/min temperature ramp up to 300ºC. The powders were then held at 300ºC for three hours. This temperature schedule was done in an atmosphere of flowing dry air. The passivation process was effective in growing a protective layer around the powder particles that reduced the amount of mass gain, as compared to unpassivated $MRE_2Fe_{14}B$ and commercial Nd-Fe-Nb-B powder, as determined by TGA.

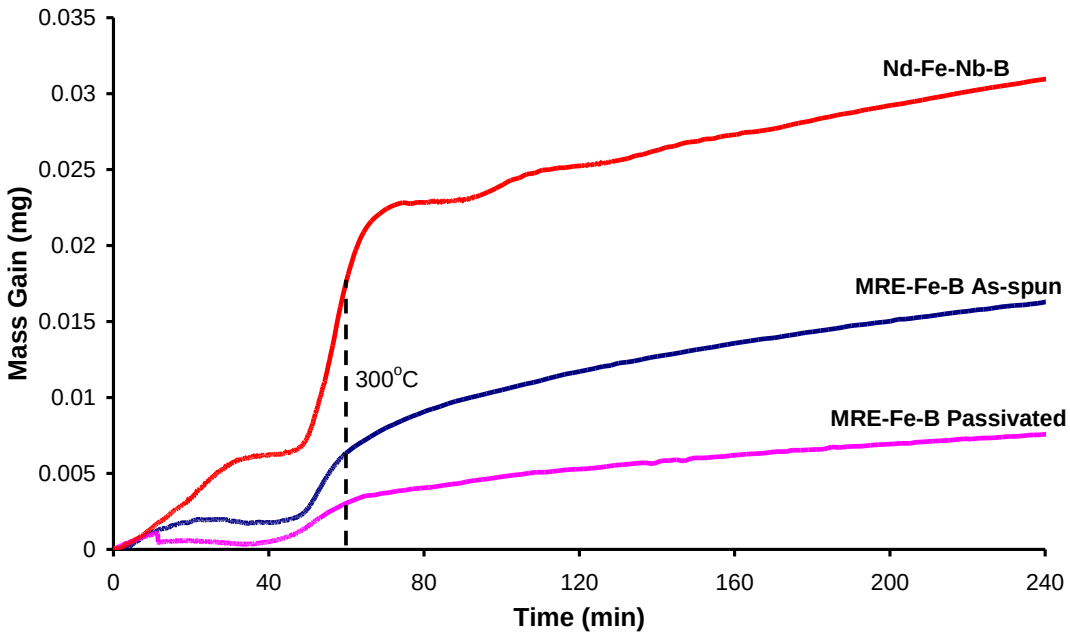

Figure 1: TGA results for $MRE_2Fe_{14}B$ in a passivated and unpassivated state with comparisons to two commercial PM alloys.

Thickness of the coating is important as it was assumed that growing the passive coating would consume rare earth from the near-surface region of each powder particle. Removal of rare earth from the magnetic phase will reduce the BH_{max} of the PM powders, decreasing the BH_{max} of the PBM. An optimal coating thickness must be determined that protects the powders but doesn't represent a significant decrease in BH_{max}. Coating thickness and composition were determined using Auger and XPS. Data from Auger, see Figure 2, shows three of the four primary elements in the passive surface coating; was fluorine, iron, and oxygen. Rare earths are hard to identify specifically with Auger due to their similar energy spectrums overlapping with each other and with associated iron peaks. The oxygen peak was the first to dissipate as the surface layers were removed by sputtering for only 15 cycles, or about 15nm. As the number of sputtering cycles increase the oxygen peak, present on the surface, disappears as the Auger scans deeper in the particle. Quantifying the difference between iron and fluoride, $(RE)F_3$ proves to be difficult for particles with a thin layer of fluorine on the

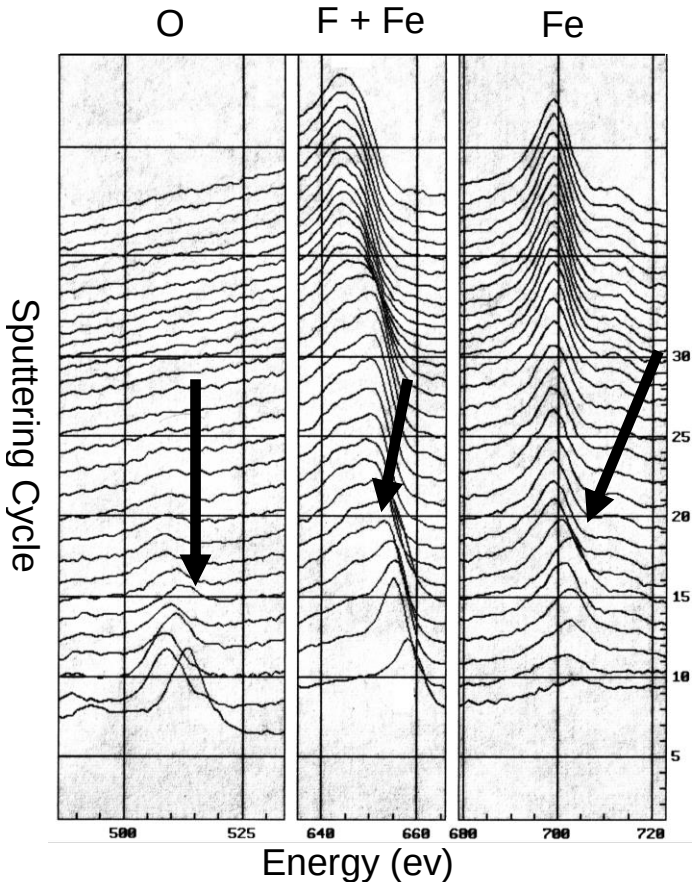

Figure 2: Auger depth profiling data showing sputtering cycle and elements present. The arrows represent termination of the oxygen and the iron fluorine peak, and the start of the iron peak

surface. A strong fluorine signal is needed because the fluorine peak shows up as a shoulder at 656eV [15] on the iron peak at 650eV [15]. Knowing this the depth to which the fluorine reacted is determined by observing drift in the iron peak. The intensity of the fluoride peak as compared to the iron peak appeared to decrease as a function of distance from the particle surface. As the fluorine peak disappeared the shoulder had less of an influence on the iron peak, causing the iron peak to shift, and change shape (at a depth of about 40nm) a good indication of coating thickness. The most encouraging result shown in Figure 3 is that the fluorine peak persisted further into the particle than the oxygen peak. This means the oxygen did not reach the $MRE_2Fe_{14}B$ phase and, therefore, will not affect the magnetic properties.

XPS was used, as well, to determine the depth and the elements that were present in the passive surface layer. This analytical method has better energy resolution, samples a larger area, and can etch the surface deeper as compared to Auger. The increased energy resolution allowed for better separation of the iron and fluorine peaks, as well as, the individual rare earth spectrums. XPS samples a much larger surface area than Auger, requiring that the small flakes be laid out in a flat mosaic pattern to make a sample that is ~1mm^2.

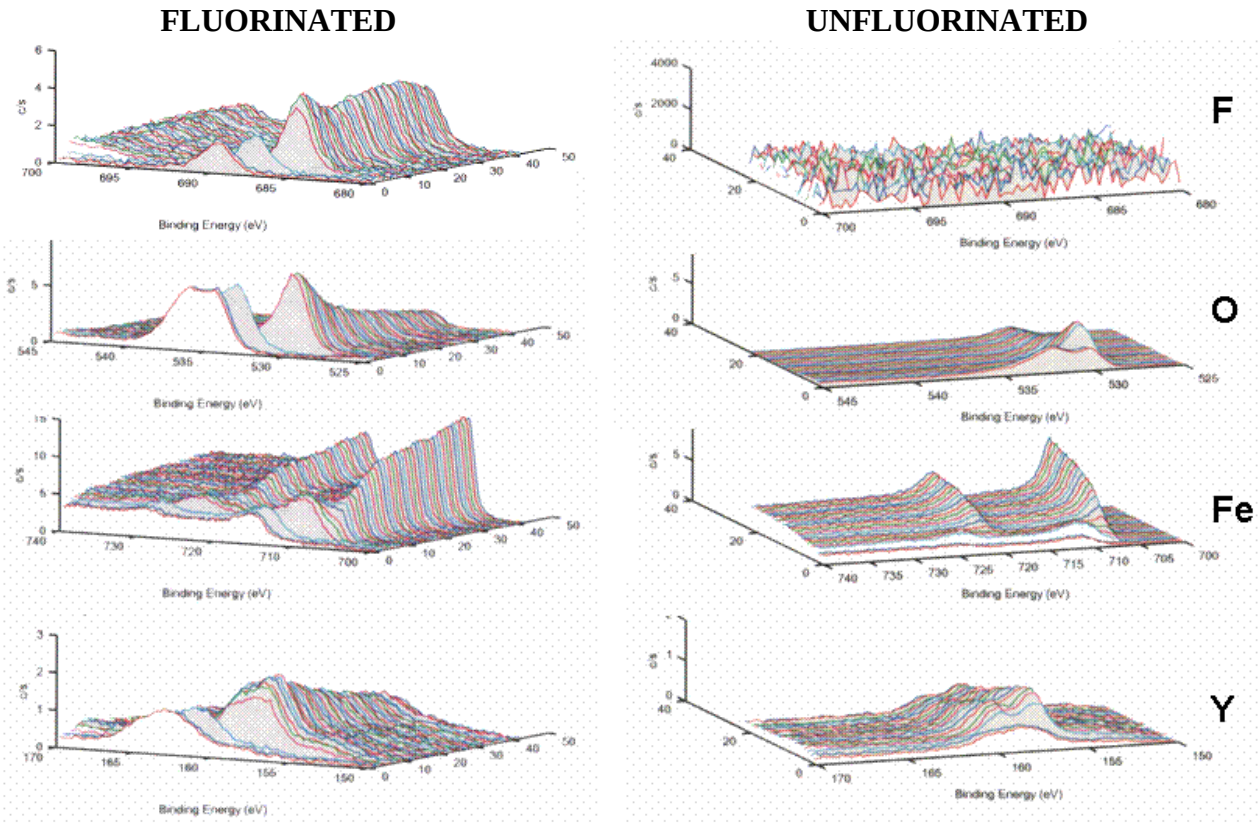

Figure 3: XPS results showing the difference in surface composition for passivated and unpassivated $MRE_2Fe_{14}B$.

XPS reasonably determined the elements contributing to the passive coating, see Figure 3. Yttrium showed up on the surface of the particles along with the iron, fluorine, and oxygen which had been previously determined with Auger. This was determined by looking at the shift in the peaks associated with yttrium. The surface peaks are shifted to a lower level as compared to the peaks determined deeper in the bulk of the material. There is a possibility of dysprosium and neodymium appearing in some small proportion in the passive layer, but XPS shows that yttrium seems to be the preferred reactant with the fluorine.

As stated earlier the thickness of the surface coating is important and it was found that the fluorine does react with the REs, especially yttrium, creating a mixture of RE-F-O, Fe-F, and O-F compounds in the passive layer. The thicknesses of the coating ranged from 5 to 80nm. Coatings in the range of 15 to 40nm were considered thick enough to prevent substantial corrosion of the particulate and reduce the associated irreversible loss of magnetic properties. This decision was based on the depth, into the particle, at which the oxygen peak had substantially reduced in intensity.

DISCUSSION

Before testing $MRE_2Fe_{14}B$ in a bonded magnet form, it needed to demonstrate a reduction in the loss of magnetic properties over a temperature range as compared to commercial $Nd_2Fe_{14}B$, as unbonded ribbon fragments. This initial test was completed in the ideal environment of a SQUID magnetometer. The BH_{max} of $MRE_2Fe_{14}B$ and commercial Nd-Fe-Nb-B were measured over a range of temperatures, terminating at the Curie temperature, to investigate the loss of BH_{max} as a function of temperature, Figure 4.

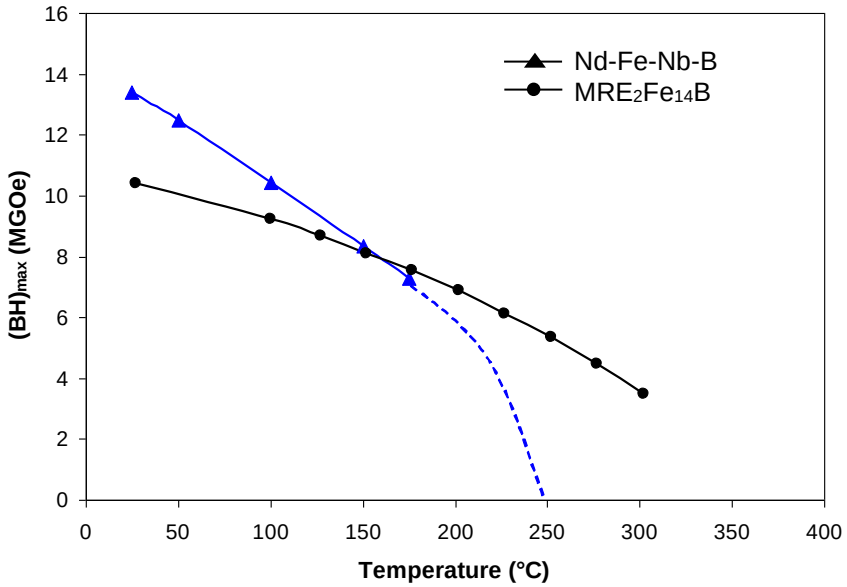

Figure 4: Temperature stability of BH_{max} of $MRE_2Fe_{14}B$ (used to make the PBMs) vs. commercially available Nd-Fe-Nb-B

The $MRE_2Fe_{14}B$ alloy $[Nd_{0.45}(YDy)_{0.25}]_{2.2}Co_{1.5}Fe_{12.5}B$ only had a 27% loss in BH_{max} as compared to a 50% loss of BH_{max} for the commercial Nd-Fe-Nb-B in the temperature range of 25 to 200°C. Thus, the ability to stabilize the BH_{max} over an increased temperature range was demonstrated. However, testing of $MRE_2Fe_{14}B$ now needed to move out of the ideal test situation (aligned ribbon pieces in the SQUID) into one that better simulates real systems. Polymer bonded PMs made with $MRE_2Fe_{14}B$ gave insight on how the powders will interact with associated binders.

Initial tests were done with unpassivated $MRE_2Fe_{14}B$ flake bonded in a compression molded epoxy matrix. This is the preferred method for making industrial STILT samples. The epoxy used is a one part dry epoxy and one part liquid that was blended with magnetic particles and compressed to densify and remove air from the sample. Samples bonded with PPS were heated to melt the PPS. Compression is used to make the molten PPS wet the surface of the particles, bonding and removing air from, the PBM.

Large amounts of air in the bonded magnets can create voids which reduce magnetic strength and act as stress concentration points.

Table 1: Comparison of the trapped air and density of the epoxy and PPS bonded magnets.

EPOXY	% Total Vol	EPOXY	% Total Vol
Nd-Fe-Nb-B	76.7%	$MRE_2Fe_{14}B$	75.1%
Epoxy	9.6%	Epoxy	9.4%
Zinc Stearate	0.5%	Zinc Stearate	0.5%
Air	13.2%	Air	15.0%
PPS	**% Total Vol**	**PPS**	**% Total Vol**
Nd-Fe-Nb-B	54.5%	$MRE_2Fe_{14}B$	65.4%
PPS	39.3%	PPS	32.1%
Air	6.2%	Air	2.5%
		$MRE_2Fe_{14}B$ FL	59.5%
		PPS	29.2%
		Air	11.4%

The data in Table 1 was measured from the PBMs used in the STILT. Using the measured weight of the PBM samples along with the known density of the materials that make up the bonded magnets, the vol% of each material that comprises the PBM was determined. The addition of air is used to make up the remainder of the volume in the calculations, should the sum of the volume of PM powder and binder be less than 100%. The difference in the loading fractions of PM flake was probably due with the variation of wetting ability of the two different binders. Epoxy has wetting characteristics that allow it to contain higher loading fractions of the PM powders than PPS. Lower loading fractions of PM powders were used when bonding with PPS. The reason the untreated $MRE_2Fe_{14}B$ PM flake bonded with PPS is loaded higher than Nd-Fe-Nb-B and $MRE_2Fe_{14}B$ FL (fluorinated $MRE_2Fe_{14}B$), is due to a change in sample size during the bonding process. A large PPS and $MRE_2Fe_{14}B$ sample was blended, and a small batch was removed from the large batch. It was assumed that the proportion of $MRE_2Fe_{14}B$ powder to PPS would be constant, but this theory did not hold true. Fortunately, the STILT is normalized, canceling out the effect of the extra flake powder in the untreated $MRE_2Fe_{14}B$ sample. The flux measurements, shown in Figures 6 and 7, during the STILT were represented as a percentage of the starting flux.

The first STILT used epoxy as the binder phase for the bonded magnets to compare commercially available $Nd_2Fe_{14}B$ PM powder to $MRE_2Fe_{14}B$ powder. The PBM containing $MRE_2Fe_{14}B$ flake powder in this test did not have a passive layer; it was bonded in an as-annealed condition. The passivation process was not developed well enough to be used on the powder samples for this test. Figure 5 displays the results of the STILT measurements for these epoxy bonded magnets.

In the epoxy bonded form made from the commercial flake powders (Nd-Fe-Nb-B) out performed the PBMs with the $MRE_2Fe_{14}B$ powder shown as $MRE_2Fe_{14}B$. Not only did Nd-Fe-Nb-B lose less flux as a function of increasing temperature, but they also had the most irreversible loss due to structural damage. Decreasing the amount of structural damage to the powders will decrease the amount of flux due to that damage. Irreversible damage is determined after the magnet has been resaturated. The difference in flux loss, and irreversible flux loss, between the $MRE_2Fe_{14}B$ PBMs and the commercial PBMs is ~1%.

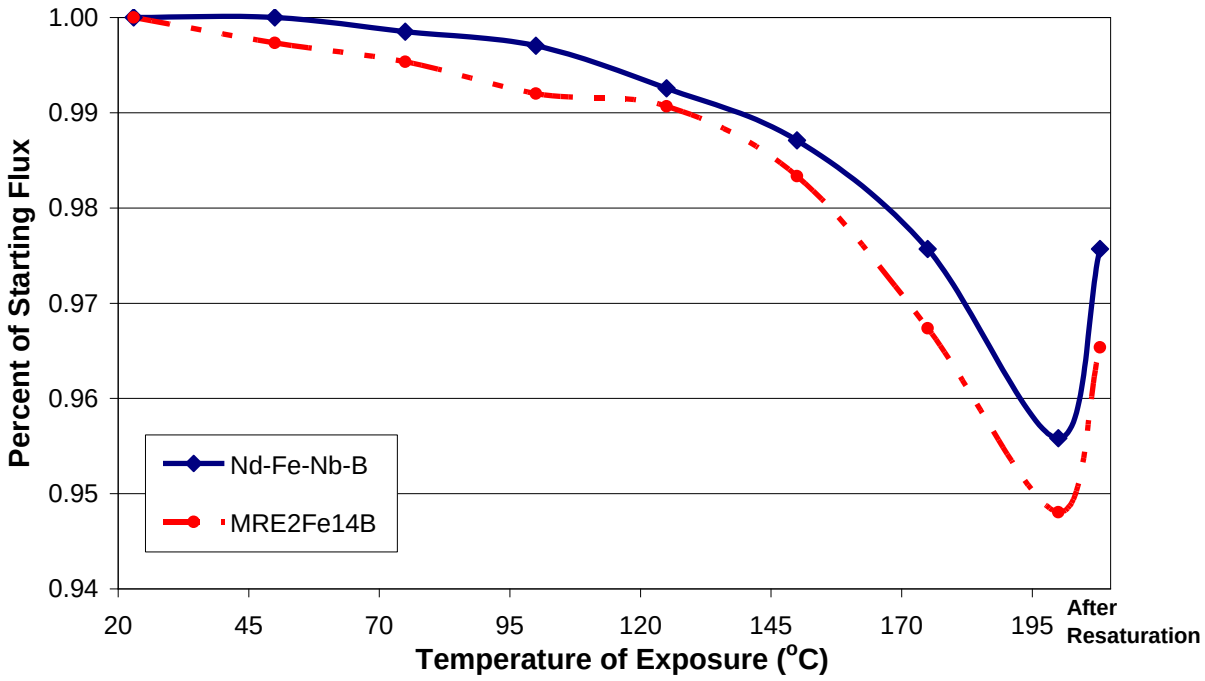

Figure 5: Epoxy bonded magnets subjected to STILT, comparing commercial Nd-Fe-Nb-B and $MRE_2Fe_{14}B$ powder.

A concern was raised about the epoxy being used as a binder. Commercial Nd-Fe-Nb-B powder came with a protective surface coating, while the $MRE_2Fe_{14}B$ powders were in the as-annealed state. The exothermic reaction that cures the epoxy may have been detrimental to the unprotected $MRE_2Fe_{14}B$ powders, increasing the magnetic loss before the start of the STILT. Also, $MRE_2Fe_{14}B$ is considered to be a high temperature 2-14-1 PM powder. The epoxy used to bond the powders for this test is not meant for the 200°C temperature seen in this test. It is possible that the epoxy will break down chemically and harm the powders as they do. To eliminate this possibility the commercial PM powder and the $MRE_2Fe_{14}B$ powder were compression molded using PPS as the binder. These possibilities reinforced the need to protect the $MRE_2Fe_{14}B$ powders from their environment.

$MRE_2Fe_{14}B$ is designed to work at higher temperatures than commercial Nd-Fe-Nb-B using the yttrium dysprosium, and cobalt additions to increase the $MRE_2Fe_{14}B$ range of operating temperatures. The epoxy and nylon binders used in commercial PBM will lose structural integrity at the increased operating temperatures. PPS is being considered the binder of choice for $MRE_2Fe_{14}B$ due to its high melting temperature. The STILT results involving PPS bonded PBMs are more encouraging than the results for the epoxy bonded PBMs, especially in the fluorinated $MRE_2Fe_{14}B$, see Figure 7.

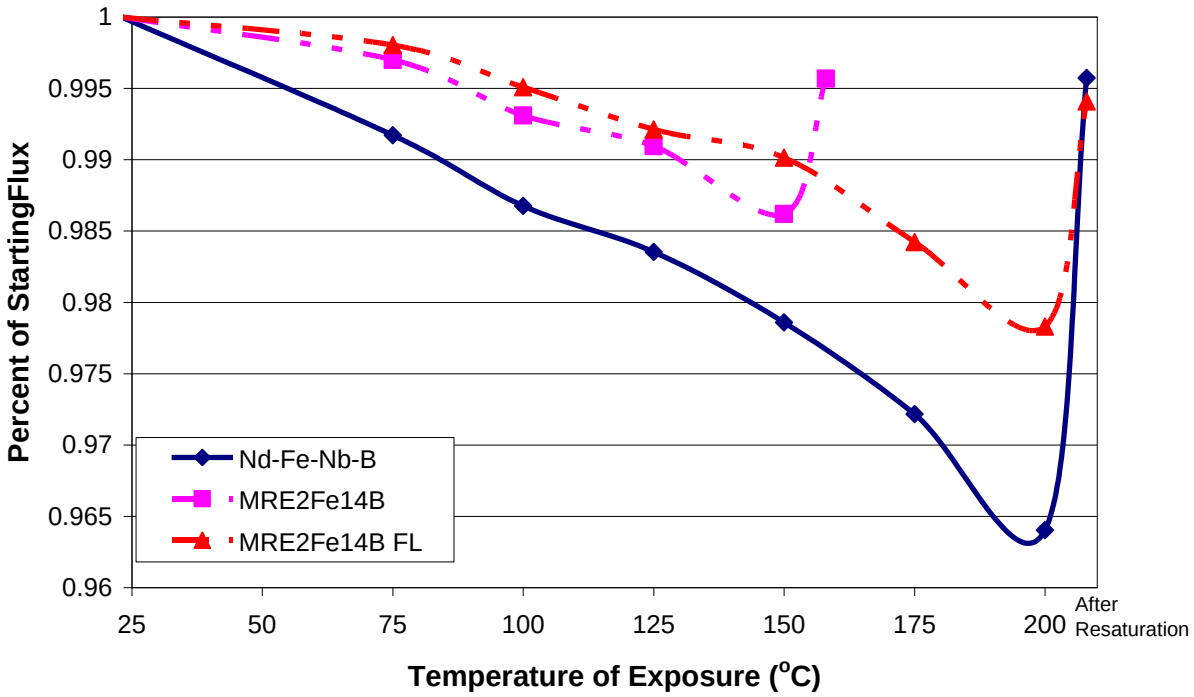

Figure 6: STILT results for bonded magnets using PPS as the binder phase for the commercial Nd-Fe-Nb-B and $MRE_2Fe_{14}B$.

The $MRE_2Fe_{14}B$, fluorinated and unfluorinated, bonded PMs showed less loss of Helmholtz flux than Nd-Fe-Nb-B powders. The passivated $MRE_2Fe_{14}B$ powder in PBM form did resist the loss of Helmholtz flux better than the commercial Nd-Fe-Nb-B PBM and the untreated $MRE_2Fe_{14}B$ PBM. The untreated $MRE_2Fe_{14}B$ PBM was not tested to 200°C as were the other two samples shown in Figure 6. Assuming that the untreated $MRE_2Fe_{14}B$ follows the same trend as seen up to 150°C it will still experience less loss than the Nd-Fe-Nb-B. However, upon resaturation it was found that the commercial alloy PBM experienced less structural damage than the fluorinated $MRE_2Fe_{14}B$. This issue has hopefully been resolved in the next iteration in the $MRE_2Fe_{14}B$ family of alloys using Ti-C to pin the grain boundaries.

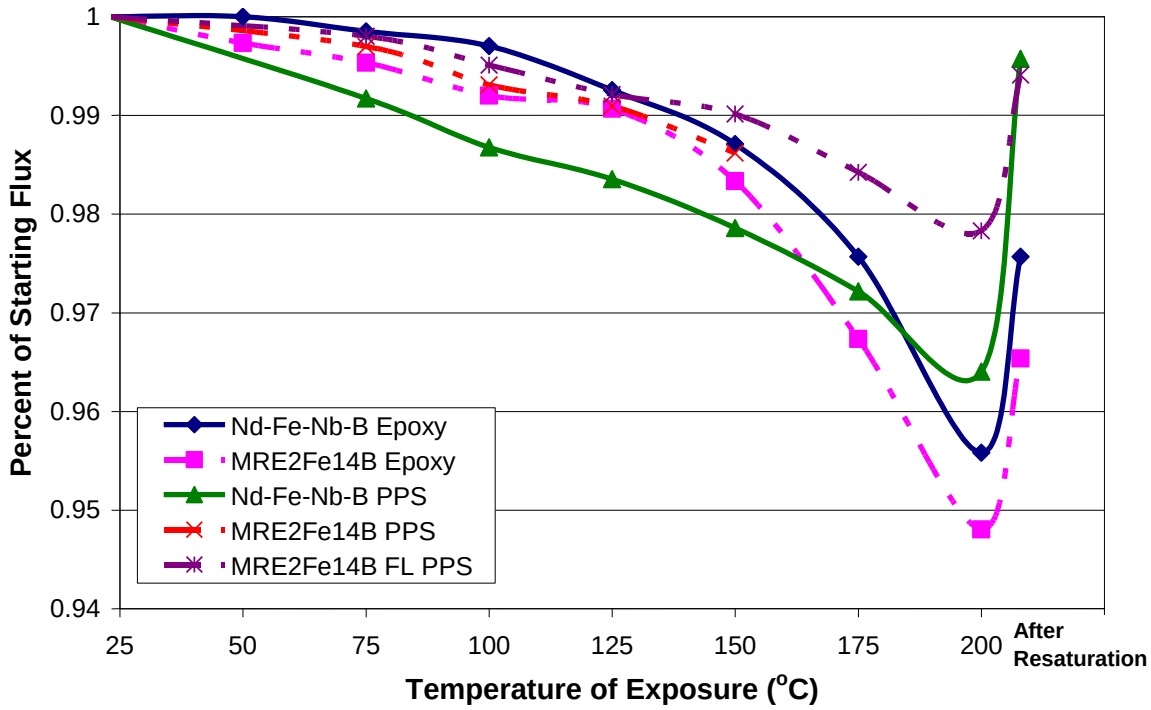

Figure 7: Direct comparison of the Epoxy and PPS bonded magnets that were subjected to STILT.

The use of PPS as a binder phase to decrease the loss of flux as a result of the STILT was successful for the $MRE_2Fe_{14}B$ PBM as compared to epoxy bonded version, see Figure 7. The effect of the epoxy binder my not be as severe as first thought but there still appears to be an effect on the $MRE_2Fe_{14}B$ powders. PPS bonded fluorinated $MRE_2Fe_{14}B$ powder was able to out perform the commercial alloy bonded in epoxy and PPS. At 200°C the fluorinated powders bonded in PPS have experienced less loss as compared to the rest of the PMBs. The commercial alloy was able to surpass the fluorinated $MRE_2Fe_{14}B$ powder in terms of permanent loss. After resaturation the commercial alloy was able to regain a slightly higher flux level indicating more structural damage in the fluorinated $MRE_2Fe_{14}B$ powders.

CONCLUSIONS

$MRE_2Fe_{14}B$, tested in ribbon fragment form, stabilized the loss BH_{max} over commercial Nd-Fe-Nb-B up to 200°C. In this ideal state and testing condition the $MRE_2Fe_{14}B$ PM alloy in melt-spun ribbon form was able to outperform commercial Nd-Fe-Nb-B. Moving to an industrial trial, $MRE_2Fe_{14}B$ must interact with binder materials in an unprotected and protected state. In the unprotected state $MRE_2Fe_{14}B$ is vulnerable to attack from the epoxy used as a binder increasing the need for a protective coating for $MRE_2Fe_{14}B$ powders. A gaseous fluorination system was developed specifically for the creation of a passive surface layer on the $MRE_2Fe_{14}B$ flake powders. Optimal coating depths were determined to be 15 to 40nm, the depth at which the oxygen signal terminates, as determined by Auger and XPS. The passive fluoride layer was proven effective against corrosion, showing the least amount of mass gain during TGA experiments. Polymer bonded magnets using PPS did not attack the $MRE_2Fe_{14}B$ powder, as was the case in the epoxy bonded samples, reducing the loss of Helmholtz flux to a level less than that seen for commercial Nd-Fe-Nb-B. The fluoride coated $MRE_2Fe_{14}B$ flake showed even less loss of Helmholtz flux as compared to the untreated $MRE_2Fe_{14}B$ powder and the commercial PM powder in an epoxy and PPS bonded magnet form.

ACKNOWLEDGMENTS

This work was supported by DOE-EE-FCVT Program, Freedom Car Initiative, USDOE-EE is acknowledged through contract no. W-7405-Eng-82. The authors are grateful for the performance of STILT testing at Arnold Magnetics Technologies of Marengo, Illinois, on an industrial partnership basis.

REFERENCES

1. A. Hütten. "Processing, Structure, and Property Relationships in Nd-Fe-B Magnets". *JOM* March (1992), 11-15.

2. D.C. Jiles. *Introduction to Magnetism and Magnetic Materials.* Chapman and Hall. London. 1991.

3. J. Bernardi, J.Fiddler, M. Sagawa, Y. Hirose. "Microstructural analysis of strip cast Nd-Fe-B alloys for high $(BH)_{max}$ magnets". *Journal of Applied Physics.* Volume 83, Number 11, 1 June 1998. 6396-6398.

4. G.C. Hadjipanayis. "Nanophase hard magnets". *Journal of Magnetism and Magnetic Materials.* 200 (1999) 373-391.

5. R.W. Gao, J.C. Zhang, D.H. Zhang, Y.Y. Dai, X.H. Meng, Z.M. Wang, Y.J. Zhang, H.Q. Liu. "Dependence of the magnetic properties on the alignment magnetic field for NdFeB bonded magnets made from anisotropic HDDR powders". *Journal of Magnetism and Magnetic Materials.* 191 (1999) 97-100.

6. D.J. Branagan, T.A. Hyde, C.H. Sellers, and R.W. McCallum. "Developing rare earth permanent magnet alloys for gas atomization". *Journal of Physics D: Applied Physics.* 29 (1996) 2376-2385.

7. A. Li, W. Li, S. Dong, X. Li. "Sintered Nd-Fe-B magnets with high strength". *Journal of Magnetism and Magnetic Materials.* 265 (2003) 331-336.

8. J. Xiao, and J. Otaigbe. "Polymer bonded magnets III. Effect of surface modification and particle size on the improved oxidation and corrosion resistance of magnetic rare earth fillers". *Journal of Alloys and Compounds.* 309 (2000) 100-106.

9. I.E. Anderson, W. Tang, R.W. McCallum. "Particulate processing and high-performance permanent magnets". *International Journal of Powder Metallurgy.* Vol 40:6 (2004) 37-60.

10. D. Goll, H. Kronmüller. "High performance permanent magnets". *Naturwissenschaften.* 87 (2000) 423-438l.

11. ISURF 02935, R.W McCallum., Y, Xu, M.J. Kramer., I.E. Anderson, K.W. Dennis "Permanent Magnet Alloy with Improved High Temperature Performance"

12. M. Seeger, D. Köhler, H. Kronmüller. "Magnetic and microstructural investigations of melt-spun Fe(NdPr)B". *Journal of Magnetism and Magnetic Materials.* 130 (1994) 165-172.

13. W. Tang, K.W. Dennis, Y. Q. Wu, M.J. Kramer, I.E. Anderson, and R.W. McCallum. "Studies of new YDy-based $R_2Fe_{14}B$ magnets for high temperature performance (R=Y+Dy+Nd)". *IEEE Transactions on Magnetics.* 40 (4), July 2004.

14. M.L. Anderson. *Surface Passivation and Electrochemical Behavior of Gas Atomized $LaNi_{4.75}Sn_{0.25}$ for Battery Applications*. Masters Thesis. Iowa State University. (2000).

15. D. Raiser, J.P. Deville. *Journal of Electron Spectroscopy and Related Phenomena*. 57, 91 (1991).

16. M.P. Seah. "Distinction between adsorbed monolayers and thicker layers in Auger electron spectroscopy", *Journal of Physics F: Metal Physics.* Vol. 3 August 1973. 1538-1547.